

Fig. 1.—

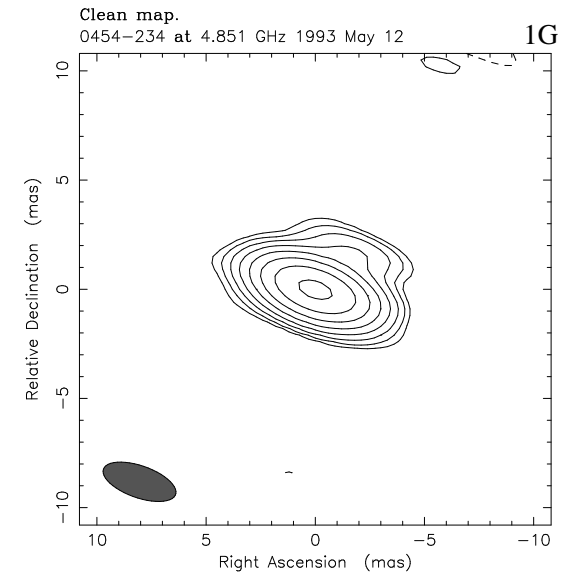
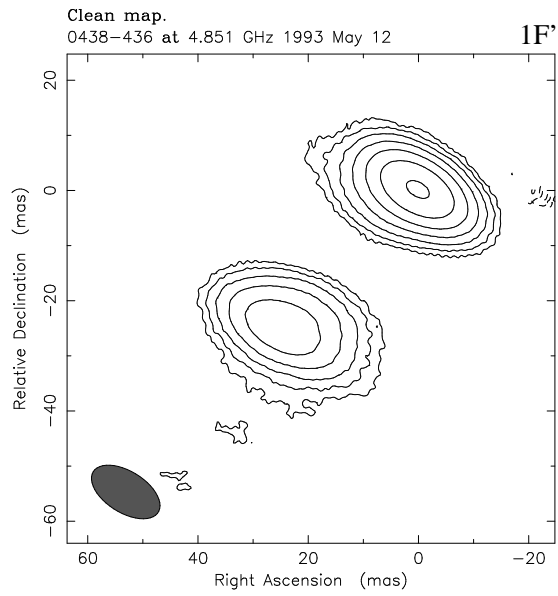
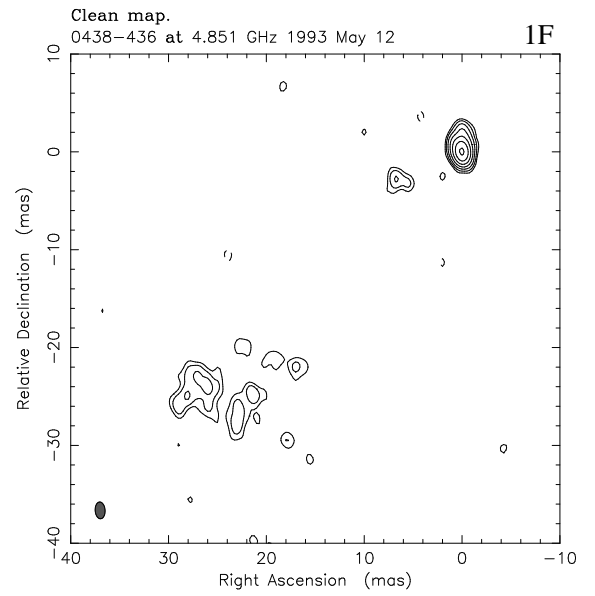
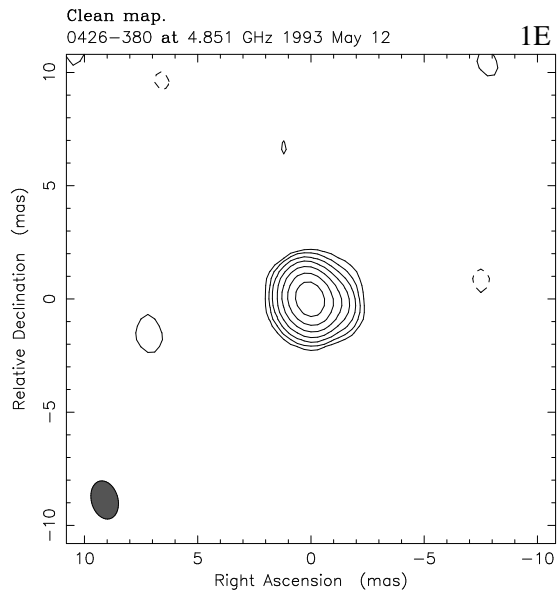


Fig. 1. — (continued)

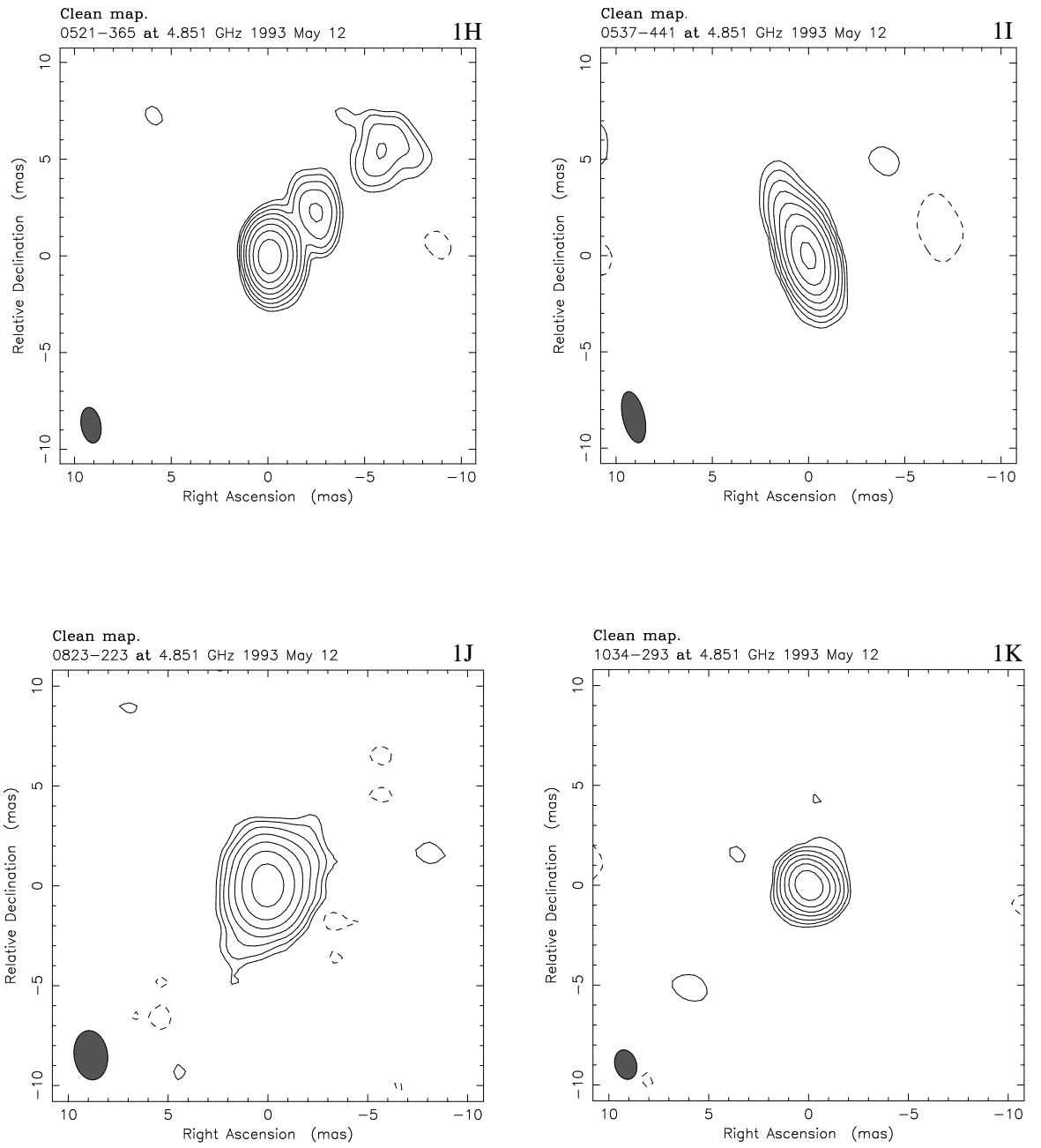


Fig. 1. — (continued)

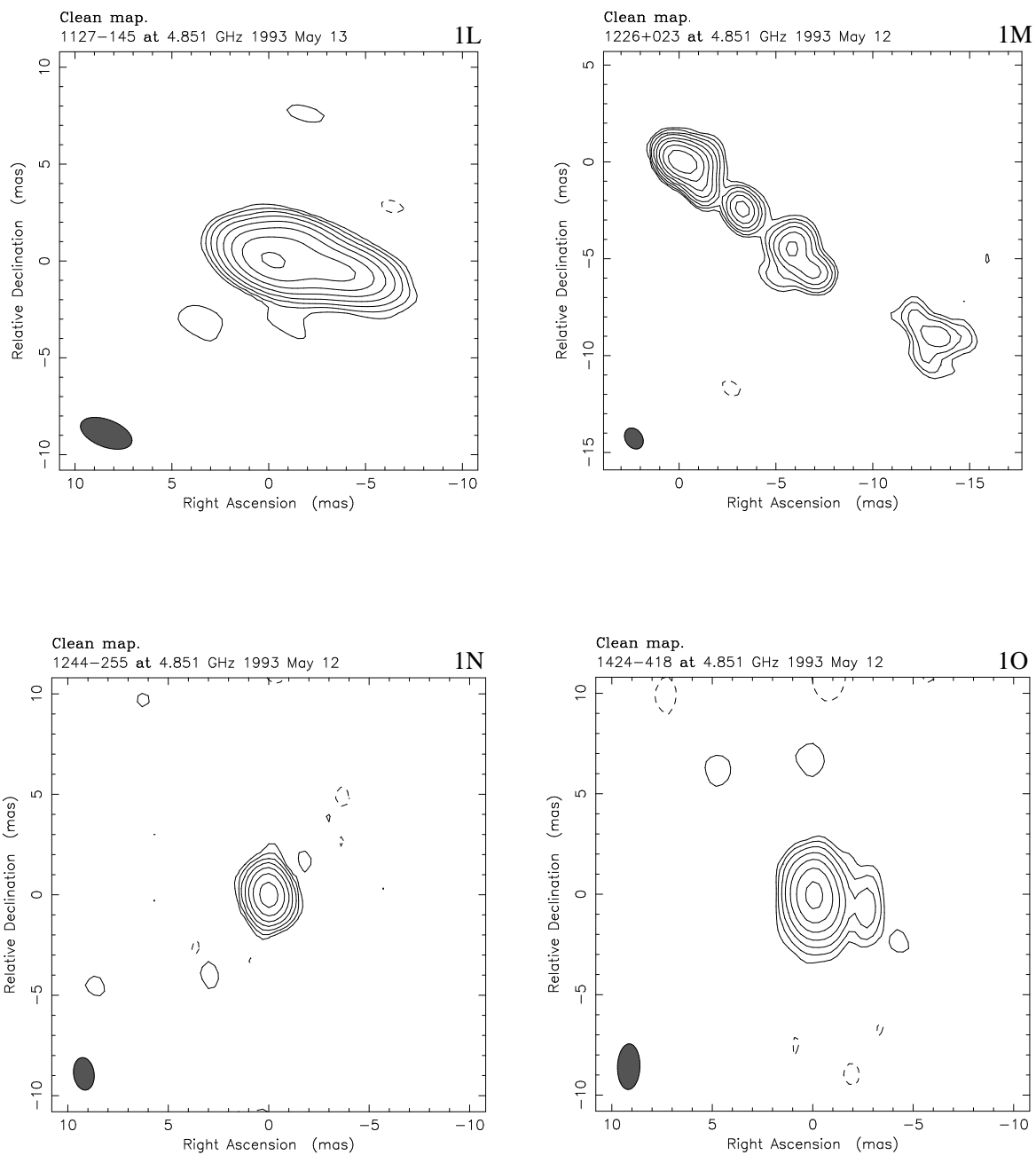


Fig. 1. — (continued)

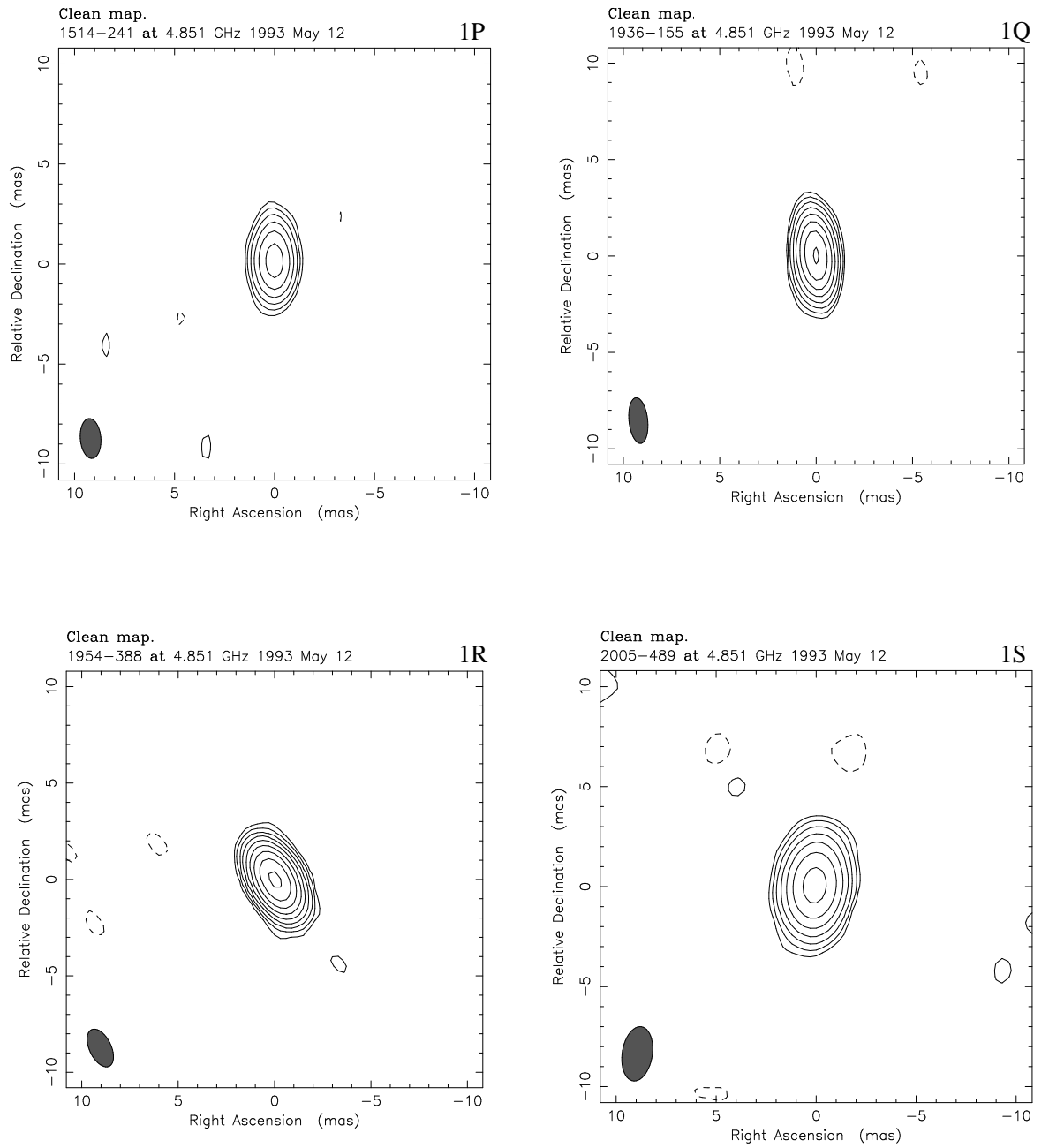


Fig. 1. — (continued)

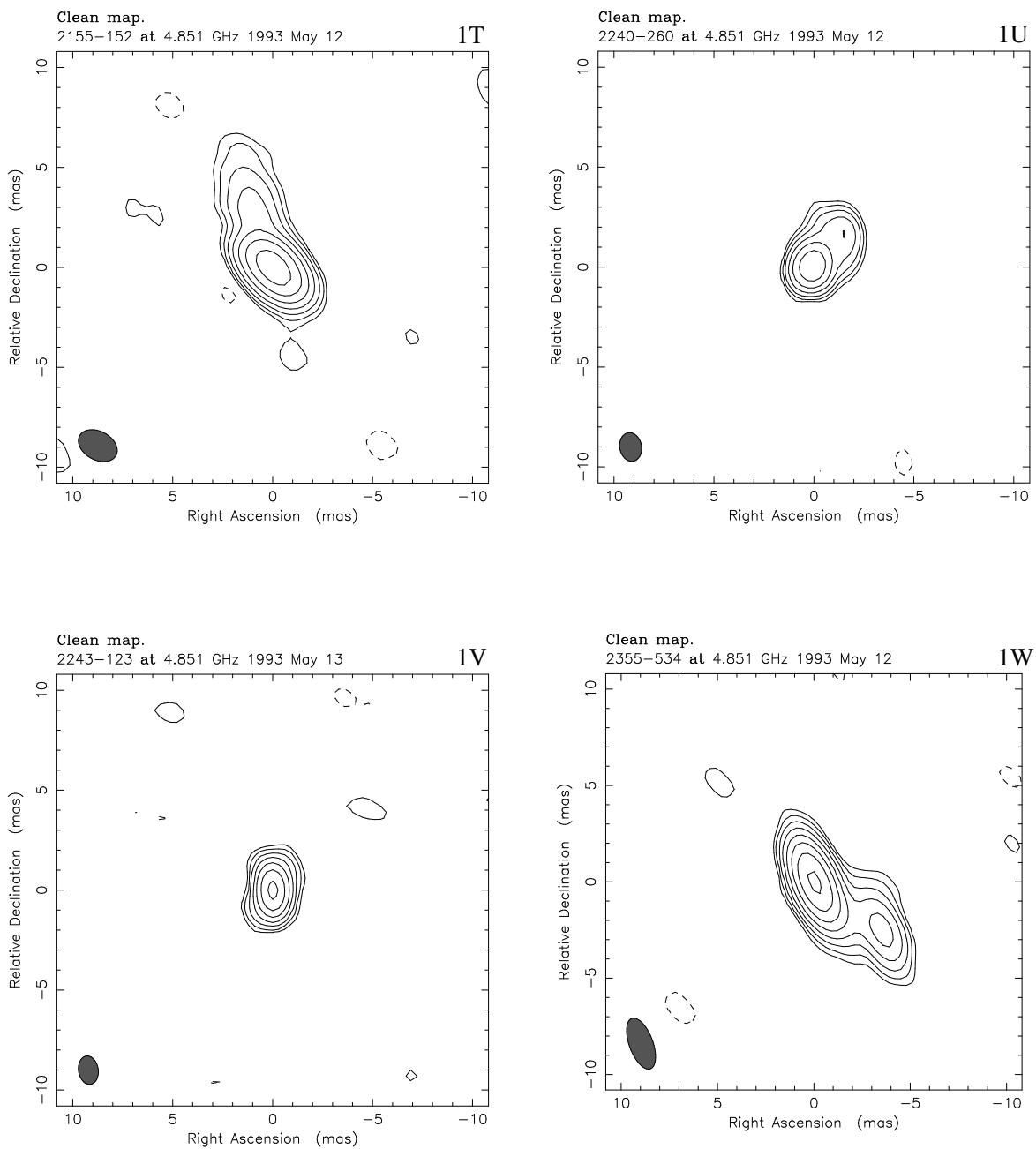


Fig. 1. — (continued)

TABLE 1. Sources Observed in 1993 May

Source Name (1)	Other (2)	R.A. (3)	Dec. (4)	z (5)	ID (6)	S_{5GHz}^t (7)
PKS 0118–272	OC–230.4	01 18 09.5395	–27 17 07.616	a 0.559	BLO	1.18
PKS 0208–512		02 08 56.9628	–51 15 07.787	1.003	HPQ	3.21
PKS 0332–403		03 32 25.2390	–40 18 24.159	1.445	HPQ	2.60
PKS 0403–132	OF–105	04 03 13.9804	–13 16 18.164	0.571	OVV	3.24
PKS 0426–380		04 26 54.7094	–38 02 52.213	a 1.030	BLO	1.14
PKS 0438–436		04 38 43.1911	–43 38 53.639	2.852	HPQ	7.00
PKS 0454–234	OF–292	04 54 57.3064	–23 29 28.356	1.009	BLO	2.00
PKS 0521–365		05 21 12.9836	–36 30 16.019	0.055	BLO	9.23
PKS 0537–441		05 37 21.0841	–44 06 44.736	0.894	BLO	3.80
PKS 0823–223		08 23 50.0776	–22 20 34.772	a 0.910	BLO	1.22
PKS 1034–293	OL–259	10 34 55.8356	–29 18 26.874	0.312	BLO	1.51
PKS 1127–145	OM–146	11 27 35.6683	–14 32 54.328	1.184	WPQ	5.46
PKS 1226+023	3C 273	12 26 33.2495	+02 19 43.458	0.158	OVV	36.70
PKS 1244–255		12 44 06.7211	–25 31 26.541	0.638	OVV	1.55
PKS 1424–418		14 24 46.6666	–41 52 54.540	1.524	HPQ	2.12
PKS 1514–241	AP LIB	15 14 45.2717	–24 11 22.582	0.049	BLO	1.94
PKS 1936–155	OV–161	19 36 36.0246	–15 32 38.828	1.657	HPQ	1.64
PKS 1954–388		19 54 39.0430	–38 53 13.599	0.626	OVV	2.00
PKS 2005–489		20 05 46.5595	–48 58 43.464	0.071	BLO	1.19
PKS 2155–152	OX–192	21 55 23.2428	–15 15 30.194	0.672	BLO	1.58
PKS 2240–260	OY–268	22 40 41.800	–26 00 12.00	0.774	BLO	1.00
PKS 2243–123	OY–172.6	22 43 39.7948	–12 22 40.407	0.630	OVV	2.38
PKS 2355–534		23 55 18.1702	–53 27 56.125	1.006	OVV	1.66

Notes to Table 1.

- (1) Source name.
- (2) Other identification.
- (3) Right ascension (B1950.0).
- (4) Declination (B1950.0).
- (5) Redshift (where there are no emission lines, ‘a’ indicates the absorption line redshift).
- (6) Optical identification (BLO=BL Lac Object, HPQ=Highly Polarized Quasar, WPQ=Weakly Polarized Quasar, OVV=Optically Violent Variable).
- (7) Total flux density in Jy at 5 GHz, from the literature.

A 5-GHz Southern Hemisphere VLBI Survey of Compact Radio Sources - II

Z.-Q. Shen¹

Harvard-Smithsonian CfA, 60 Garden Street, Cambridge, Massachusetts 02138
and Shanghai Astronomical Observatory, 80 Nandan Road, Shanghai 200030, China

T.-S. Wan

Shanghai Astronomical Observatory, 80 Nandan Road, Shanghai 200030, China

J. M. Moran

Harvard-Smithsonian CfA, 60 Garden Street, Cambridge, MA 02138

D. L. Jauncey, J. E. Reynolds, A. K. Tzioumis, R. G. Gough, R. H. Ferris and M. W. Sinclair
Australia Telescope National Facility, CSIRO, Epping, NSW 2121, Australia

D.-R. Jiang, X.-Y. Hong and S.-G. Liang

Shanghai Astronomical Observatory, 80 Nandan Road, Shanghai 200030, China

P. G. Edwards

The Institute of Space and Astronautical Science, Sagamihara, Kanagawa 229, Japan

M. E. Costa²

Physics Department, University of Western Australia, Nedlands, WA 6009, Australia

S. J. Tingay³

Mount Stromlo and Siding Spring Observatories, ACT 2611, Australia

P. M. McCulloch, J. E. J. Lovell⁴ and E. A. King⁵

Department of Physics, University of Tasmania, Hobart, Tasmania 7001, Australia

G. D. Nicolson

Hartebeesthoek Radio Astronomy Observatory, Krugersdorp 1740, South Africa

D. W. Murphy, D. L. Meier, and T. D. van Ommen⁶

Jet Propulsion Laboratory, California Institute of Technology, Pasadena, California 91109

G. L. White

Physics Department, University of Western Sydney, Nepean, NSW 2747, Australia

¹Present address: Institute of Astronomy and Astrophysics, Academia Sinica, P.O. Box 1-87, Nankang, Taipei 115, Taiwan

²Present address: University of Tasmania, Hobart, Tasmania 7001, Australia

³Present address: Jet Propulsion Laboratory, California Institute of Technology, Pasadena, California 91109

⁴Present address: The Institute of Space and Astronautical Science, Sagami-hara, Kanagawa 229, Japan

⁵Present address: Australia Telescope National Facility, CSIRO, Epping, NSW 2121, Australia

⁶Present address: Antarctic CRC, University of Tasmania, G.P.O. 252C Hobart, Tasmania, Australia

ABSTRACT

We report the results of a 5-GHz southern-hemisphere snapshot VLBI observation of a sample of blazars. The observations were performed with the Southern Hemisphere VLBI Network plus the Shanghai station in 1993 May. Twenty-three flat-spectrum, radio-loud sources were imaged. These are the first VLBI images for 15 of the sources. Eight of the sources are EGRET (> 100 MeV) γ -ray sources. The milliarcsecond morphology shows a core-jet structure for 12 sources, and a single compact core for the remaining 11. No compact doubles were seen. Compared with other radio images at different epochs and/or different frequencies, 3 core-jet blazars show evidence of bent jets, and there is some evidence for superluminal motion in the cases of 2 blazars. The detailed descriptions for individual blazars are given. This is the second part of a survey: the first part was reported by Shen *et al.* (1997).

1. Introduction

Blazar is the collective name for BL Lac objects, optically violent variables and highly polarized quasars, all of which share extreme observational properties that distinguish them from other active galactic nuclei. These properties include strong and rapid variability, high optical polarization, weak emission lines, and compact radio structure (cf. Impey 1992). About 200 blazars have been identified (cf. Burbidge & Hewitt 1992). A possible explanation for the blazar phenomenon within a unified scheme for active galactic nuclei is that their emission is beamed by the relativistic motion of the jets traveling in a direction close to the observer's line of sight. This beaming argument is strengthened by the recent CGRO (Compton Gamma Ray Observatory) discovery that most of the detected high-latitude γ -ray sources are blazars (e.g. Dondi & Ghisellini 1995). A comprehensive theoretical review of these sources has been made by Urry & Padovani (1995).

Blazars are an important class of active galactic nuclei because they are thought to be sources with relativistic jets seen nearly end-on. Such sources generally have very compact, flat-spectrum radio cores, which are appropriate for VLBI study. Pearson & Readhead (1988) have undertaken a survey of a complete sample consisting of 65 strong northern-hemisphere radio sources. They provided the first well-defined morphological classification scheme, based primarily on the large-scale radio structure and radio spectra of the sources.

Most surveys to date, however, including the recent Caltech–Jodrell Bank VLBI Surveys (Polatidis *et al.* 1995; Thakkar *et al.* 1995; Xu *et al.* 1995; Taylor *et al.* 1994; Henstock *et al.* 1995), have been restricted to northern-hemisphere sources. For example, all the confirmed superluminal radio sources, except the well-known equatorial source 3C 279 (1253–055), are in the northern sky (Vermeulen & Cohen 1994). This reflects the paucity of southern VLBI observations, the notable exceptions being the systematic one-baseline surveys by Preston *et al.* (1985) and Morabito *et al.*

(1986), and the more extensive SHEVE survey (Preston *et al.* 1989 and references therein).

Since 1992 we have been carrying out a program to address this deficiency, using VLBI at 5 GHz to study southern radio sources. In an earlier paper (Shen *et al.* 1997, hereafter Paper I), we reported the results from the first observing session in 1992 November, and presented images of 20 strong sources selected on the basis of their correlated fluxes on intercontinental baselines. In 1993 May we observed a second sample of southern sources, which is the subject of this paper.

Section 2 introduces this blazar sample; Section 3 briefly describes the observations and data reduction procedures; Section 4 presents the results; the summary and conclusions are presented in Section 5.

Throughout the paper, we define the spectral index, α , by the convention $S_\nu \propto \nu^\alpha$, and assume $H_0 = 100 \text{ km s}^{-1} \text{ Mpc}^{-1}$ and $q_0 = 0.5$.

2. The Blazar Sample

We selected our sample of southern blazars from Table 1 of Burbidge & Hewitt (1992), which was based on the 2.7-GHz Parkes Survey of Bolton *et al.* (1979) and the 5-GHz survey of Kühr *et al.* (1981). The sample is defined by the following criteria:

1. Declination: $-55^\circ < \delta < -10^\circ$,
2. total flux density at 5.0 GHz: $S_{5.0\text{GHz}}^t > 1.0 \text{ Jy}$,
3. radio spectral index between 2.7 and 5.0 GHz: $\alpha_{2.7\text{GHz}}^{5.0\text{GHz}} \geq -0.5$.

Of the 218 sources listed by Burbidge & Hewitt (1992), 24 meet the above criteria. These include PKS 1334–127, PKS 1504–166 and PKS 1519–273, which were observed in the first session (Paper I) and not re-observed here. The remaining 21 sources are listed in Table 1, along with 2 additional sources that were included in the observing run: 3C 273 (1226+023) and PKS 1127–145, a radio-loud quasar. PKS 0823–223 has the lowest galactic latitude of this sample, with $b \sim 9^\circ$; for all other sources, $|b| > 17^\circ$.

Seven blazars (PKS 0332–403, PKS 0426–380, PKS 0438–436, PKS 0521–365, PKS 1034–293, PKS 1226+023 and PKS 2234–123) belong to the 36-source sample described in Paper I, but were not observed in 1992 November. Also, 6 sources (PKS 0208–512, PKS 0521–365, PKS 0537–441, PKS 1127–145, PKS 1226+023 and PKS 1424–418) have been detected by the EGRET (Energetic Gamma-Ray Experiment Telescope) on board the CGRO (Mattox *et al.* 1997), and two blazars (PKS 0454–234 and PKS 2005–489) were marginally detected (Thompson *et al.* 1995; Fichtel *et al.* 1994). Their names, positions, redshifts, optical identifications and flux densities at 5 GHz are provided in Table 1.

3. Observations

Our VLBI observations were carried out within 48 hours on 1993 May 12–13, using the radio telescopes at Hartebeesthoek (South Africa), Hobart (Australia), Mopra (Australia), Parkes (Australia), Perth (Australia), and Shanghai (China). The observing parameters of these stations are given in Table 2. One element of the Australia Telescope Compact Array (Narrabri, Australia) also observed, but due to a configuration problem during recording, no useful data were obtained.

This second snapshot session followed a similar observing mode and data processing procedure as the first session (see Paper I), so only a brief outline is given here. All 23 sources in Table 1 were observed in snapshot mode, i.e., three to five 30-minute scans were obtained. Data were recorded in Mark II format with 2-MHz bandwidth and left-circular polarization (IEEE convention). The cross-correlation of the data was carried out on the JPL/Caltech Mark II Processor in 1994.

Post-correlation data reduction was done at the Harvard-Smithsonian Center for Astrophysics, using the NRAO AIPS and Caltech VLBI analysis packages. A global fringe-fitting procedure consisting of AIPS tasks was run at a solution interval of 2.5 minutes. The 64-m Parkes telescope was selected as the reference station. Fringes were found for all 23 sources. The visibility data were phase self-calibrated with a 10-second solution interval and a point-source model in AIPS. The data averaging, editing, imaging, deconvolution, and self-calibration were then performed within DIFMAP, a part of the Caltech VLBI Package (Shepherd, Pearson & Taylor 1994). Natural weighting was applied and only a constant gain factor correction was implemented in the amplitude-calibration. Finally, we ran the MODELFIT program in the Caltech VLBI Package to fit the closure phases and amplitudes of the calibrated data on each source, in order to obtain a quantitative description of its structure. Up to three Gaussian components were fitted for 22 sources, while 6 components were used in the case of 3C 273, the strongest source in the sample. In all cases, we feel that these models reasonably characterize the fundamental features observed.

4. Results

The naturally weighted images for the 23 radio sources are presented in Figure 1. In each image, the size of the restoring beam is shown as a cross-hatched ellipse in the lower-left corner. The lowest contour level in each image is three times the rms noise level. The rms noise in the images is a few mJys per beam for all the sources except 3C 273, for which the noise level was 18 mJy/beam. The image parameters (peak flux density, restoring beam and contour levels) are listed in Table 3. The results of the model-fitting are given in Table 4, together with the peak brightness temperature for each model component in the rest frame of the source, calculated following the method described in Paper I.

PKS 0118–272 (OC–230.4, Fig. 1A)

This is a BL Lac object with a tentative emission-line redshift of $z=1.62$ (Adam 1985 and

references therein). A lower limit of $z > 0.559$ was suggested from several absorption lines (Falomo 1991; Stickel, Fried, & Kühr 1993). Strong optical variations of 100% within three days have been reported (Falomo, Scarpa, & Bersanelli 1994). PKS 0118–272 is also highly optically polarized (Impey & Tapia 1988; Mead *et al.* 1990).

A 20-cm VLA observation revealed a complex structure, while at 6 cm the source exhibited at least three components within $1''$ (Perley 1982). A single-baseline 2.3-GHz VLBI observation yielded a correlated flux density of 0.53 ± 0.05 , corresponding to a visibility of 0.5 ± 0.2 (Preston *et al.* 1985). Our observations showed a resolved core with diffuse surrounding emission. The data were fitted by a single N–S elongated Gaussian component with a flux density of 0.55 Jy. However, the core accounts for only half the total flux density of the source, which supports the presence of two or three additional weak features in the vicinity. The source has a spectral index of 0.02 at millimeter wavelengths (Steppe *et al.* 1988), with a total flux density of 0.60 Jy at 230 GHz.

PKS 0208–512 (Fig. 1B)

This flat-spectrum radio source has a redshift $z=1.003$ (Peterson *et al.* 1976). It is classified as a highly polarized quasar or blazar by Impey & Tapia (1988, 1990). It was the second southern AGN (after 3C 279) detected at γ -ray energies (Bertsch *et al.* 1993; Blom *et al.* 1995), with one of the hardest photon spectral indices (von Montigny *et al.* 1995; Chiang *et al.* 1995).

No detailed arcsecond-scale structure of the source has been reported in the literature. The SHEVE experiment at 2.3 GHz described it as a Gaussian component with a minimum nuclear flux density of 2.5 Jy (Preston *et al.* 1989). A 5-GHz VLBI image from 1992 November revealed a core-jet structure along a position angle of 233° (Tingay *et al.* 1996).

The image from our observation in 1993 May is in excellent agreement with that of Tingay *et al.* (1996). The source has a compact 2.8-Jy core, and a 0.3-Jy jet component at an angular separation of 1.7 mas and a position angle of 234° from the central core. A nearly flat spectral index of 0.15 for the core is estimated from the 2.3- and 5.0-GHz results. The derived brightness temperature is 1.9×10^{12} K, close to the value of 1.2×10^{12} K in Tingay *et al.* (1996). We note that the γ -ray emission is also thought to be beamed due to its short variation time-scale (of tens of days) and high observed luminosity (of 10^{48} ergs sec^{-1} for isotropic emission) (Bertsch *et al.* 1993). Further study of this source may contribute to a better understanding of the correlation between γ -ray emission and radio radiation. A lower limit to the Doppler factor is 10.2 using the ROSAT X-ray observation ($0.22 \mu\text{Jy}$ at 1 Kev) (Doni & Ghisellini 1995). This implies superluminal motion in the compact core, having an upper limit of 6° to the viewing angle. Comparison of the 1992 and 1993 images taken 6.5 months apart suggests a proper motion of 0.6 ± 0.7 mas yr^{-1} , corresponding to an apparent speed of 17 ± 20 c. Further high-accuracy VLBI measurements are needed to confirm its superluminal motion.

PKS 0332–403 (Fig. 1C)

This source is a highly polarized quasar (Impey & Tapia 1988; 1990). It has an inverted

spectrum that peaks at around 5 GHz (Shimmings *et al.* 1971) and could be classified as a gigahertz-peaked-spectrum (GPS) source (cf. O’Dea, Baum, & Stanghellini 1991). Its redshift of $z=1.445$ has been widely used in the literature without clear justification. This value is from *Catalogue of Quasi Stellar-Objects*, edited by Barbieri, Capaccioli, & Zambon (1975), in which the reference was incorrect. A new measurement should be made to confirm its redshift.

The arcsecond structure of PKS 0332–403 is dominated by an unresolved core from 6- and 20-cm VLA observations (Perley 1982). Preston *et al.* (1985) detected a correlated flux of 0.17 ± 0.03 Jy, in contrast to a total flux at 2.3 GHz of 4.0 ± 0.4 Jy. Single-baseline measurements at 2.3 and 8.4 GHz were also made by Morabito *et al.* (1986). Our high-resolution image revealed a strong compact core and a weak unresolved feature to the east (see Table 4). The derived Doppler factor from the ROSAT 0.1–2.4 KeV observations (Brinkmann, Siebert, & Boller 1994) is greater than 3.6.

PKS 0403–132 (OF–105; Fig. 1D)

This quasar has strong emission lines and a redshift of $z=0.571$ (Lynds 1967). It is an optically violent variable source (Bolton *et al.* 1966) and has a variable, modest linear polarization (Moore & Stockman 1981; Impey & Tapia 1988). There is evidence of variability at X-ray energies (Blumenthal, Keel, & Miller 1982).

The VLA 20-cm image of Wardle *et al.* (1984) shows a core-jet structure, with an unresolved nucleus extending on opposite sides, and a jet lying at a position angle of 23° . The nucleus remains unresolved at 6 cm (Morganti, Killeen, & Tadhunter 1993), with a possible weak extension (Wills & Browne 1986). The model from high-resolution VLBI data at 2.3 GHz exhibits two unresolved components, which have a flux-density ratio of 5 and a separation of 580 mas along a position angle of 48° (Preston *et al.* 1989).

Our VLBI image at 5 GHz revealed only a compact core, with no other component emission. The weak secondary component in the 2.3-GHz model may be resolved, or have a steep spectrum, or have decayed since 1982. The core component can be fitted by a single 0.5 mas by 0.3 mas Gaussian component with a 0.85-Jy flux density and a brightness temperature of 5.0×10^{11} K. This high brightness is consistent with the moderate variation of the source at radio (Romero, Benaglia, & Combi 1995), optical (Bolton *et al.* 1966), and X-ray (Blumenthal, Keel, & Miller 1982) wavelengths.

PKS 0426–380 (Fig. 1E)

This is a BL Lac object with no detected emission lines, and an absorption redshift of $z_{abs}=1.030$ (Stickel *et al.* 1993). PKS 0426–380 has an optical polarization less than 3% (Impey & Tapia 1990). VLA observations at 20 cm show a 2.7-arcsecond extension from the compact core to the position angle of -24° (Perley 1982). Single-baseline VLBI observations gave correlated flux densities of 0.70 and 0.90 Jy, at frequencies of 2.3 and 8.4 GHz, respectively (Morabito *et al.* 1986).

The data of PKS 0426–380 were modeled by a Gaussian component extended along a position angle of 111° . Using the absorption redshift and the upper limit to the 1 keV X-ray flux density from ROSAT observations (Brinkmann *et al.* 1994), the estimated lower limit to the Doppler boosting factor is 3.1. Our model gives a brightness temperature of 7×10^{11} K for the core.

PKS 0438–436 (Figs. 1F & 1F')

This extremely luminous radio quasar has an emission-line redshift of $z=2.852$ with some absorption lines superimposed (Morton, Savage, & Bolton 1978). Optically, PKS 0438–436 is faint with variable polarization (e.g. Rusk 1990; Fugmann & Meisenheimer 1988; Impey & Tapia 1988, 1990). It has a complex radio spectrum, flat at low frequencies, but very steep above 5 GHz. The flux density at 1.4 GHz is known to vary by 10% over a period of four months. The polarization also varies in degree and position angle (Luna *et al.* 1993). It has been detected by the IRAS satellite (Neugebauer *et al.* 1986), and also has significant soft X-ray absorption (Wilkes *et al.* 1992). Both of these properties are unusual for a quasar with such a high redshift. No γ -ray detection was reported from the EGRET all-sky survey. Perley (1982) identified a secondary component 2.2 arcseconds away from the core at a position angle of 15° . VLBI observations at 2.3 GHz showed a core-jet structure: two 1.9 Jy circular components separated by 35 mas at a position angle of -43° (Preston *et al.* 1989).

Our 5-GHz VLBI observation confirms the two-component structure described above, with the same separation and orientation of the two components, to within the errors. To facilitate a comparison, we convolved the 5.0-GHz data with the 2.3-GHz SHEVE beam ($13.9 \text{ mas} \times 7.5 \text{ mas}$ at a position angle of 58°) to obtain the image shown in Fig. F', which has a peak flux density of 1.6 Jy/beam. The lowest contour level is 23 mJy/beam, with a factor of 2 between adjacent contours. It is clear that the northwest component is stronger and more compact than the one to the southeast. We identify the northwest component as the core, which has a brightness temperature of 7.8×10^{11} K, 100 times higher than that of the other component. Actually, as can be seen in Fig. 1F, the southeast component has been heavily resolved at 5 GHz. The core size agrees well with the analysis of early VLBI measurement at 2.3 GHz, which showed a variable component smaller than 1 mas in diameter (Gubbay *et al.* 1977). There is about a 120° difference in position angle between the arcsecond- and mas-scale structures.

PKS 0454–234 (OF–292; Fig. 1G)

This is listed as a BL Lac object (Ledden & O'Dell 1985) due to its featureless optical spectrum (Wilkes *et al.* 1983). An initial redshift determination of 1.009 (Wright, Ables, & Allen 1983) was later refined as $z=1.003$ (Stickel, Fried, & Kühr 1989). It is a highly polarized quasar with optical polarization up to 27% (Wills *et al.* 1992). PKS 0454–234 was detected at marginal significance by EGRET at >100 MeV γ -ray energies (Thompson *et al.* 1993b).

PKS 0454–234 was detected in the 2.3-GHz TDRSS experiment on a 1.8 earth-diameter baseline (Linfield *et al.* 1989), and in a 22-GHz ground survey on a baseline of 10,000 km (Moellenbrock *et al.* 1996). Our 5-GHz VLBI image shows an asymmetrical morphology with a

strong core and a compact jet-like component to the northwest at a position angle of -62° . The brightness temperature of the core as derived from our model is about 6×10^{11} K. A Doppler beaming factor of 5.3 is estimated using the X-ray flux density at 1 KeV and core structural parameters. For comparison, a value of 3.6 was derived from the variability time-scale (Dondi & Ghisellini 1995).

PKS 0521–365 (Fig. 1H)

This radio source has been identified with an N galaxy (Bolton *et al.* 1965). A redshift of $z=0.055$ has been measured from both absorption features and emission lines (Danziger *et al.* 1979). It is one of 5 radio sources (cf. Crane *et al.* 1993) which have prominent optical counterparts to their radio jets (Danziger *et al.* 1979; Folomo 1994 and references therein). The Hubble Space Telescope has resolved the optical jet structure (Macchetto *et al.* 1991). High optical polarization has been measured in the jet and the nucleus as well (Sparks, Miley, & Macchetto 1990 and references therein). This suggests a synchrotron origin of the optical radiation. It has strong X-ray emission (Pian *et al.* 1996) and has been marginally detected above 100 MeV by EGRET (Fichtel *et al.* 1994; Lin *et al.* 1995).

Its arcsecond-scale radio structure is dominated by an extended lobe to the southeast, rather than by the compact core itself (Wardle, Moore, & Angel 1984; Keel 1986; Slee *et al.* 1994). A radio jet follows closely, in direction and extent, the optical jet to the northwest (Ekers *et al.* 1989). The magnetic fields inferred from the polarization measurements at the optical and radio wavelengths are parallel to the jet direction in the jet, and perpendicular to the jet in the core. From 2.3-GHz VLBI observations, the core was modeled as a circular source 1.4 mas in diameter, with a flux density of 1 Jy (Preston *et al.* 1989).

VLBI observations at 5.0 and 8.4 GHz revealed a 0.5-Jy jet component at a position angle of 310° (Tingay *et al.* 1996). No apparent motion could be determined from four-epoch measurements over a period of one year.

Our high-resolution data disclosed a second jet component near the compact core. The parameters of these components are listed in Table 4. The two jet components are aligned with the VLA jet ($302^\circ \pm 2^\circ$, Keel 1986) and optical jet ($311^\circ \pm 2^\circ$, Cayatte & Sol 1987). No beaming effect is needed for the core brightness temperature of 1.7×10^{11} K. This is consistent with the nondetection of superluminal motion. The γ -ray luminosity between 100 MeV and 5 GeV is about 3.2×10^{44} ergs sec^{-1} (Lin *et al.* 1995), the second lowest in the sample of gamma-ray-loud AGN. All of these observations suggest a large angle in PKS 0521–365 between the ejection direction and the line of sight. Pian *et al.* (1996) derived a viewing angle of 30° with bulk Lorentz factor of 1.2. This leads to a predicted jet-counterjet ratio of 64, assuming a jet spectral index of -1.0 . However, none of the existing VLBI images reveal any feature on the opposite side of the core. Further high dynamic range VLBI images will help constrain the modelling of this source.

PKS 0537–441 (Fig. 1I)

This is a $z=0.894$ (Peterson *et al.* 1976) transition object between classical BL Lac objects and quasars (Cristiani 1985; Maraschi *et al.* 1985; Giommi, Ansari, & Micol 1995). It has displayed substantial variability at X-ray energies (Treves *et al.* 1993 and references therein), and has shown similar variation time scales and amplitudes at wavelengths ranging from infrared to X-ray (Tanzi *et al.* 1986), suggesting that these emissions may originate from the same spatial region. The source is also a strong variable EGRET γ -ray source (Thompson *et al.* 1993a).

On the arcsecond scale the source is core-dominated with a bright secondary component separated by 7.2 arcseconds at a position angle of 305° (Perley 1982). The SHEVE 2.3-GHz observation showed a 4.2-Jy core with a diameter of 1.1 mas (Preston *et al.* 1989). Recent VLBI observations at 4.9 and 8.4 GHz (Tingay *et al.* 1996) show a jet-like component to the north of the compact core.

Our 5-GHz VLBI image confirmed the asymmetric core-jet structure, in good agreement with the results from Tingay *et al.* (1996). However, the VLBI jet component differs by 70° in position angle from the VLA secondary component (Perley 1982). The VLBI core has a brightness temperature of 8.6×10^{11} K. Unfortunately, the existing VLBI data were insufficient to determine the proper motion of the jet in this EGRET-identified radio source.

PKS 0823–223 (Fig. 1J)

This is a BL Lac object (Wright *et al.* 1979; Wilkes *et al.* 1983) with an absorption redshift of $z_{abs}=0.910$ (Falomo 1990 and references therein). It shows high optical polarization (Impey & Tapia 1990). No γ -ray emission was detected by EGRET (Fichtel *et al.* 1994).

VLA observations show a diffuse structure on arcsecond scales at 20 cm (Perley 1982). Our 6-cm VLBI image can be modeled by a 1.2 mas by 0.3 mas Gaussian component with a flux density of 0.4 Jy. The earlier total flux-density measurement of 1.8 Jy (Impey & Tapia 1990) and VLA structure imply that PKS 0823–223 has some extended structure which is resolved and therefore undetected by our VLBI observations.

PKS 1034–293 (OL–259; Fig. 1K)

This is a BL Lac object with a redshift of $z=0.312$ (Stickel *et al.* 1989 and references therein) and which displays high optical polarization of up to 14% (Wills *et al.* 1992). PKS 1034–293 is a strong millimeter-wavelength source with a variable flux density between 1.0 Jy to 3.0 Jy (Steppe *et al.* 1988, 1992, 1993).

Previous VLBI observations described PKS 1034–293 as a core-dominated, strong compact radio source (Robertson *et al.* 1993; Morabito *et al.* 1986). The TDRSS experiment at 2.3 GHz fitted it as a 0.58-Jy, 0.44-mas circular Gaussian component (Linfield *et al.* 1989).

Our VLBI data were fitted with an elliptical Gaussian component 0.8 mas by 0.5 mas, with a flux density of 1.5 Jy. The derived brightness temperature is 2.5×10^{11} K, consistent, within

errors, with the measurement of 4.6×10^{11} K from the 22-GHz ground survey (Moellenbrock *et al.* 1996) and 9.2×10^{11} K from the 2.3-GHz TDRSS (Linfield *et al.* 1989).

PKS 1127–145 (OM–146; Fig. 1L)

This is a high-redshift quasar with broad emission lines at $z=1.184$ (Wilkes *et al.* 1983; Wilkes 1986) and absorption lines at $z_{abs}=0.313$ (Bergeron & Boisse 1991). It has low optical polarization (Impey & Tapia 1990; Wills *et al.* 1992; Tornikoski *et al.* 1993) and is not an optically violently variable source (Pica *et al.* 1988; Bozayan, Hemenway, & Argue 1990). It has been identified in the second EGRET catalog at energies above 100 MeV (Thompson *et al.* 1995).

PKS 1127–145 was unresolved in VLA observations (Perley 1982). It is strong and compact, and was detected at both 2.3 and 15 GHz on TDRSS baselines larger than 14,000 km (Linfield *et al.* 1989, 1990). Two-epoch VLBI observations at 1.7 GHz (Padielli *et al.* 1986; Romney *et al.* 1984) found that PKS 1127–145 was slightly extended to the north. No structural variation between the two epochs (1.7 years) was seen. A proper motion of 0 ± 0.02 in the source was reported by Vermeulen & Cohen (1994). The 5-GHz image of Wehrle *et al.* (1992) resolved the source into two compact components plus a weak extension to the northeast.

Our VLBI observation revealed two Gaussian components. The brighter component, with a flux density of 1.9 Jy, is larger than the weaker (1.1 Jy) component (see Table 4). These two components have similar brightness temperatures of $\sim 1.3 \times 10^{11}$ K. They are probably related to two components of nearly equal strength resolved by Wehrle *et al.* (1992), and possibly to the east–west structure observed at 1.7 GHz (Padielli *et al.* 1986; Romney *et al.* 1984). We find no evidence of a northeast extension seen by Wehrle *et al.* (1992). We note that early VLBI experiments at 18, 13 and 6 cm indicated at least three distinct components in the source, implying source evolution (Kellermann *et al.* 1971; Weiler & de Pater 1983).

PKS 1226+023 (3C 273; Fig. 1M)

This well-known radio source has been identified with a thirteenth magnitude object at a redshift of $z=0.158$ (Hazard, Mackey, & Shimmins 1963; Schmidt 1963). It shows optical variation, which was first analyzed by Smith and Hoffleit (1963), but does not have high optical polarization (Appenzeller 1968). It is very bright across the wavebands from radio to γ -ray. It was the only γ -ray source known before the CGRO observations (Swanenburg *et al.* 1978; Bignami *et al.* 1981), and one of the first two extragalactic sources detected by EGRET (Mattox *et al.* 1997 and references therein).

The large-scale structure from the VLA and MERLIN shows a compact, flat-spectrum core and a single jet extending about 23 arcseconds from the core at a position angle of 222° (Conway *et al.* 1993). This source has received considerable attention since the VLBI technique became available, due mainly to its intensity and variability. Multi-frequency VLBI observations show a bright core and a number of jet components extending toward the southwest (e.g. Davis *et al.* 1991; Zensus *et al.* 1988).

Our VLBI observation of this equatorial quasar has a good north–south resolution with a beam of 1.6 mas by 0.88 mas at a position angle of 33° . We fitted six components, labeled 1 through 6, to the data. The strong component 1 at the eastern end is identified as the core. No counterjet is visible. Components 2 to 6 are jet components, or knots in the continuous jet, which have a similar position angle of $\sim 230^\circ$ and increasing distance to the core (from 1.9 mas for component 2 to 15.2 mas for component 6). Along this position angle, there is a distinct emission gap between components 5 and 6. Such morphology is consistent with other published results (e.g. Zensus *et al.* 1988). Comparison with earlier observations enables us to identify the components in our image with those seen previously: our components 2, 3 and 4 are respectively C_{10} , C_9 and C_8 (Abraham *et al.* 1994). Our component 5 is C_{7a} (Cohen *et al.* 1987). The more extended component 6 in our image is more difficult to identify, and may be C_6 (Unwin *et al.* 1985; Zensus 1987; Charlot, Lestrade, & Boucher 1988) or possibly a mixture of C_6 and other components (such as C_5 , C_4 , or even C_3) (see Cohen *et al.* 1987, Unwin *et al.* 1985). Such identification is in good agreement with the observational picture of the evolution of the different components in 3C 273 (see Abraham *et al.* 1996).

PKS 1244–255 (Fig. 1N)

This source is a blazar (Bersanelli *et al.* 1992), having violent optical variation (Bozayan *et al.* 1990 and references therein) and high optical polarization (Impey & Tapia 1988, 1990). It has strong emission lines corresponding to a redshift of $z=0.638$ (Falomo *et al.* 1994).

VLBI observations yielded correlated flux densities of 0.48 Jy at 2.3 GHz, 1.01 Jy at 8.4 GHz (Morabito *et al.* 1986), and 0.91 Jy at 22 GHz (Moellenbrock *et al.* 1996). Our VLBI image shows a simple compact core elongated at a position angle of 116° , with a brightness temperature of 5.6×10^{11} K. This is consistent with the measurement of $>4.0 \times 10^{11}$ K from the 22-GHz survey.

PKS 1424–418 (Fig. 1O)

This is a highly optically polarized quasar (Impey & Tapia 1988, 1990). An accurate redshift measurement of $z=1.524$ was made by Stickel *et al.* (1989). Data on PKS 1424–418 from the 2.3-GHz SHEVE observations were modeled by two circular components separated by 23 mas (Preston *et al.* 1989). Our VLBI image shows two components separated by ~ 3 mas. Assuming the stronger component is the core, the position angle of the weaker component is 260° , significantly different from the reported value for the two 2.3-GHz components of $236/284^\circ$ (Preston *et al.* 1989). There is a difference in alignment of 90° between the VLBI and VLA structures. Using the model results, we obtain a very flat spectral index of -0.04 for the central core. For comparison, we calculated a spectral index of 0.20 from the correlated flux density measured at 2.3 and 8.4 GHz (Robertson *et al.* 1993). An asymmetry was also inferred from their data.

PKS 1514–241 (AP LIB; Fig. 1P)

This source is a classical BL Lac object (Strittmatter *et al.* 1972). The redshift is $z=0.0486$, based upon both absorption lines and emission lines (Rodgers & Peterson 1977 and references

therein). It has been characterized as an optically violent variable (Carini *et al.* 1991; Bozyan *et al.* 1990; Webb *et al.* 1988) and a highly polarized quasar (Wills *et al.* 1992).

This source shows a core-jet morphology on arcsecond scales in 6- and 20-cm VLA images (Morganti *et al.* 1993; Antonucci & Ulvestad 1985; Ulvestad, Johnston, & Weiler 1983). A component 0.2 arcsecond from the core at a position angle of 120° was reported by Perley (1982).

Our VLBI image of this BL Lac object shows only a single component, 1.2 mas by 0.6 mas in size, with elongation in the north–south direction, and a flux density of 1.53 Jy. The brightness temperature is 1.1×10^{11} K, which is consistent with the value of $\sim 1.5 \times 10^{11}$ K from the 22-GHz survey (Moellenbrock *et al.* 1996).

PKS 1936–155 (OV–161; Fig. 1Q)

This is a blazar with high optical polarization (Fugmann & Meisenheimer 1988) and a high redshift of $z=1.657$ (Jauncey *et al.* 1984). It has a very steep spectrum between 1.4 and 2.7 GHz, and a flat spectrum between 2.7 and 5.0 GHz, and probably to 8.4 GHz (Quiniento & Cersosimo 1993; Impey & Tapia 1990).

VLA 6-cm observations showed the source to be unresolved, with a flux density of 0.72 Jy (Neff, Hutchings, & Gower 1989). Our VLBI image shows a single component 0.6 mas by 0.5 mas in size, elongated in the north–south direction, with a flux density of 0.97 Jy. A slight extension to the southeast can be seen from the map. The compact core has a brightness temperature of 4.7×10^{11} K, compared to $>2.5 \times 10^{11}$ K from the 22-GHz survey (Moellenbrock *et al.* 1996).

PKS 1954–388 (Fig. 1R)

This is an optically violent variable (Gilmore 1980) with a redshift of $z=0.626$ (Browne, Savage, & Bolton 1975). It also has a high optical polarization up to 11% (Impey & Tapia 1988, 1990). VLA observations at 20 cm showed a diffuse structure (Perley 1982). Previous VLBI observations showed the presence of a compact core at 2.3 GHz (Preston *et al.* 1985). Our VLBI image shows a single compact component 0.4 mas by 0.3 mas in size, with a flux density of 1.9 Jy. The calculated brightness temperature is 1.2×10^{12} K.

PKS 2005–489 (Fig. 1S)

This source is a BL Lac object at a redshift of $z=0.071$ (Falomo *et al.* 1987). It is one of two objects with low optical polarization in the 1-Jy BL Lac object sample (Stickel *et al.* 1993; Stickel *et al.* 1991). It is one of the few extragalactic sources detected in the EUV band (Marshall, Fruscione, & Carone 1995). Its detected X-ray flux is far in excess of a simple power-law extrapolation from lower frequency measurements, and is among the three or four brightest BL Lac objects having violent optical variation (Wall *et al.* 1986; Bozyan *et al.* 1990). It has shown large amplitude, short time-scale variability among different X-ray observations (e.g. Della Ceca *et al.* 1990; Elvis *et al.* 1992; Brinkmann *et al.* 1994; Ghosh & Soundararajperumal 1995). It was only marginally detected by EGRET (Fichtel *et al.* 1994; Thompson *et al.* 1995).

Our VLBI data shows a simple compact component, 1.0 mas by 0.2 mas in size, with a flux density of 0.92 Jy and a corresponding brightness temperature of 2.6×10^{11} K.

PKS 2155–152 (OX–192; Fig. 1T)

This is an OVV BL Lac object (Craine *et al.* 1976; Bozayan *et al.* 1990) displaying very high optical polarization (Brindle *et al.* 1986; Impey & Tapia 1990) and a redshift of $z=0.672$ (White *et al.* 1988; Stickel *et al.* 1989). On the arcsecond scale, the source exhibits a triple structure with an extension of 6 arcseconds along the north–south direction (Weiler & Johnston 1980; Perley 1982; Wardle *et al.* 1984). Our VLBI image reveals a core-jet morphology. The unresolved core is strong, with a high brightness temperature of $>6.7 \times 10^{11}$ K. The source axis seems to be well aligned on both the mas and arcsecond scales.

PKS 2240–260 (OY–268; Fig. 1U)

This BL Lac object has a redshift of $z=0.774$ (Stickel *et al.* 1993). High optical polarization has also been observed in the source (Impey & Tapia 1988, 1990). Our VLBI data shows a core-jet structure, of which the stronger component has a flux density of 0.54 Jy. The secondary component, at a distance of 2.2 mas and a position angle of 314° , is 0.12 Jy. We identify the core with the stronger component, although both components have similar brightness temperatures.

PKS 2243–123 (OY–172.6; Fig. 1V)

This is an optically violent variable and a highly polarized quasar (Impey & Tapia 1988, 1990; Wills *et al.* 1992), with a redshift of $z=0.630$ (Browne *et al.* 1975). This radio source has also been classified as a GPS source, because its spectrum shows a turnover at ~ 2.3 GHz (Cersosimo *et al.* 1994).

VLA observations exhibited an unresolved core with a 4-arcsecond extended component at a position angle of 40° (Perley 1982; Browne & Perley 1986; Morganti *et al.* 1993). Observations on a single long baseline measured correlated flux densities of 0.78 Jy and 1.23 Jy, at 2.3 and 8.4 GHz, respectively (Morabito *et al.* 1986).

Our VLBI data can be fitted as a compact core with a flux density of 2.28 Jy, and size of 1.1 mas by 0.4 mas, with a corresponding brightness temperature of 4.0×10^{11} K. The core has a north–south elongation. We note that there is a depression at the east–west side of the core, which might indicate the emergence of a new component. A second epoch VLBI observation in 1995 October showed a resolved structure, with a jet-like component to the south, 1.12 mas from the strong central component (Shen, Hong, & Wan 1998). A proper motion of 0.22 mas yr^{-1} is estimated, which corresponds to an apparent superluminal motion of $4.6c$ in the jet.

PKS 2355–534 (Fig. 1W)

This is an optically violent and highly polarized source (Impey & Tapia 1988, 1990) with a high redshift of $z=1.006$ (Jauncey *et al.* 1984). There have been no previous measurements of the radio structure. Our image shows two components with similar size but different flux densities.

The stronger component, which may be the core, has a brightness temperature of 3.5×10^{11} K. The second component is located at a distance of 4.9 mas at a position angle of 235° .

5. Summary

In this paper we have defined a sample of southern-hemisphere core-dominated blazars. Of the 24 blazars in the sample, 3 were observed earlier with the same array. The other 21 in the sample and 2 other sources were observed in 1993 May with the Southern VLBI Network plus the Shanghai radio telescope. This is part of the Southern Hemisphere 5-GHz VLBI Survey project, the aim of which is to improve the study of southern extragalactic radio sources (see Paper I). Our study also adds significantly to the number of sources whose structures can be compared on arcsecond (kpc) and milliarcsecond (pc) scales (Table 5). The misalignment of jet-like structures on these scales is an important unsolved problem for the understanding of compact sources.

The main conclusions presented in this paper can be summarized as follows:

1. We have detected and imaged all 23 radio sources, of which 15 are first-epoch VLBI images. These are PKS 0118–272, PKS 0332–403, PKS 0426–380, PKS 0454–234, PKS 0823–223, PKS 1034–293, PKS 1244–255, PKS 1514–241, PKS 1936–155, PKS 1954–388, PKS 2005–489, PKS 2155–152, PKS 2240–260, PKS 2243–123 and PKS 2355–534.
2. Most of the blazars are resolved and display simple morphology, with 12 having core-jet structures and 11 having single-core structures. Observations with increased sensitivity will probably reveal many more core-jet structures (e.g. 2243–123). We have compared our VLBI images with other radio images. Only 3 (PKS 0438–436, PKS 0537–441 and PKS 1226+023) of the 12 core-jet blazars were found to have curved jets. Superluminal motion was inferred from two-epoch observations for 2 sources (PKS 0208–512, PKS 2243–123).
3. Eight of these blazars (PKS 0208–512, PKS 0454–234, PKS 0521–365, PKS 0537–441, PKS 1127–145, PKS 1226+023, PKS 1424–418 and PKS 2005–489) have been detected at > 100 MeV γ -ray energies. Together with the other 5 EGRET sources observed in 1992 November (Paper I), a total of 13 southern γ -ray-loud blazars have now been imaged by our survey project. A systematic study of the VLBI properties of these γ -ray blazars and comparison with other non- γ -ray sources will improve our understanding of the beaming characteristics in blazars and the properties of EGRET sources.

This work was supported at Shanghai Astronomical Observatory by grants from the National Program for the Enhancement of Fundamental Research. Part of this research was carried out at the Jet Propulsion Laboratory, California Institute of Technology, under contract with the National Aeronautics and Space Administration. We would like to thank M. Reid, M. Birkinshaw

and C. Carilli for helpful discussions. We thank an anonymous referee for helpful and constructive comments. Z.-Q. Shen acknowledges the receipt of a Smithsonian Pre-doctoral Fellowship. The Australia Telescope National Facility is funded by the Australian Government for operation as a national facility by the CSIRO. Our search of the literature was greatly assisted by the NASA/IPAC Extragalactic Database (NED), which is operated by the Jet Propulsion Laboratory, California Institute of Technology, under contract with the National Aeronautics and Space Administration.

REFERENCES

- Abraham, Z., Carrara, E. A., Zensus, J. A., & Unwin, S. C. 1994, in Compact Extragalactic Radio Sources, eds. J. A. Zensus and K. I. Kellermann (National Radio Astronomy Observatory, Greenbank), 87-90
- Abraham, Z., Carrara, E. A., Zensus, J. A., & Unwin, S. C. 1996, *A&AS*, 115, 543-549
- Adam, G. 1985, *A&AS*, 61, 225-235
- Antonucci, R. R. J., & Ulvestad, J. S. 1985, *ApJ*, 294, 158-182
- Appenzeller, I. 1968, *ApJ*, 151, 769-770
- Barbieri, C., Capaccioli, M., & Zambon, M. 1975, *Mem. Soc. Astron. Italiana*, 46, 461-499
- Bergeron, J., & Boisse, P. 1991, *A&A*, 243, 344-366
- Bersanelli, M., Bouchet, P., Falomo, R., & Tanzi, E. G. 1992, *AJ*, 104, 28-39
- Bignami, G. F., *et al.* 1981, *A&A*, 93, 71-75
- Bertsch, D. L., *et al.* 1993, *ApJ*, 405, L21-L24
- Blom, J. J., *et al.* 1995, *A&A*, 298, L33-L36
- Blumenthal, G. R., Keel, W. C., & Miller, J. S. 1982, *ApJ*, 257, 499-508
- Bolton, J. G., Clarke, M. E., & Ekers, R. D. 1965, *Australian J. Phys.*, 18, 627
- Bolton, J. G., Savage, A., & Wright, A. E. 1979, *Aust. J. Phys. Astroph. Supp*, 46, 1-17
- Bolton, J. G., Shimmins, A. J., Ekers, J., Kinman, T. D., Lamia, E., & Wirtanen, C. A. 1966, *ApJ*, 144, 1229-1231
- Bozayan, E. P., Hemenway, P. D., & Argue, A. N. 1990, *AJ*, 99, 1421-1434
- Brindle, C., Hough, J. H., Bailey, J. A., Axon, D. J., & Hyland, A. R. 1986, *MNRAS*, 221, 739-768
- Brinkmann, M., Siebert, J., & Boller, T. 1994, *A&A*, 281, 355-374
- Browne, I. W. A., Savage, A., & Bolton, J. G. 1975, *MNRAS*, 173, 87
- Browne, I. W. A., & Perley, R. A. 1986, *MNRAS*, 222, 149-166
- Burbidge, G., & Hewitt, A. 1992, in Variability of Blazars, eds. E. Valtaoja and M. Valtonen (Cambridge University Press, Cambridge), 4-38
- Carini, M. T., Miller, H. R., Noble, J. C., & Sadun, A. C. 1991, *AJ*, 101, 1196-1201
- Cayatte, V., & Sol, H. 1987, *A&A*, 171, 25-32
- Cersosimo, J. C., Lebron Santos, M., Cintron, S. I., & Quiniento, Z. M. 1994, *ApJS*, 95, 157-161

- Charlot, P., Lestrade, J.-F., & Boucher, C. 1988, in IAU Symp. 129, The Impact of VLBI on Astrophysics and Geophysics, eds. M. J. Reid and J. M. Moran (Kluwer, Dordrecht), 33-34
- Chiang, J., *et al.* 1995, ApJ, 452, 156-167
- Cohen, M. H., Zensus, J. A., Biretta, J. A., Comoretto, G., Kaufmann, P., & Abraham, Z. 1987 ApJ, 315, L89-L92
- Conway, R. G., Garrington, S. T., Perley, R. A., & Biretta, J. A. 1993, A&A, 267, 347-362
- Craine, E. R., *et al.* 1976, Astrophys. Lett., 17, 123-125
- Crane, P., *et al.* 1993, ApJ, 402, L37-L40
- Cristiani, S. 1985, IAU Circulars, No. 4027
- Danziger, I. J., Fosbury, R. A. E., Goss, W. M., & Ekers, R. D. 1979, MNRAS, 188, 415-419
- Davis, R. J., Unwin, S. C., & Muxlow, T. W. B. 1991, Nature, 354, 374-376
- Della Ceca, R., Palumbo, G. G. C., Persic, M., Boldt, E. A., de Zotti, G., & Marshall, E. E. 1990, ApJS, 72, 471-550
- Dondi, L., & Ghisellini, G. 1995, MNRAS, 273, 583-593
- Ekers, R. D., *et al.* 1989, MNRAS, 236, 737-777
- Elvis, M., Plummer, D., Schachter, J., & Fabbiano, G. 1992, ApJS, 80, 257-303
- Falomo, R., Maraschi, L., Tanzi, E. G., & Treves, A. 1987, ApJ, 318, L39-L41
- Falomo, R. 1990, ApJ, 353, 114-117
- Falomo, R. 1991, AJ, 102, 1991-1993
- Falomo, R. 1994, ESO Messenger, 77, 49-52
- Falomo, R., Scarpa, R., & Bersanelli, M. 1994, ApJS, 93, 125-143
- Fichtel, C. E., *et al.* 1994, ApJS, 94, 551-581
- Fugmann, W., & Meisenheimer, K. 1988, A&AS, 76, 145-156
- Ghosh, K. K., & Soundararajperumal, S. 1995, ApJS, 100, 37-68
- Gilmore, G. 1980, MNRAS, 190, 649-667
- Giommi, P., Ansari, S. G., & Micol, A. 1995, A&AS, 109, 267-291
- Gubbay, J., Legg, A. J., Robertson, D. S., Nicolson, G. D., Moffet, A. T. & Shaffer, D. B. 1977, ApJ, 215, 20-35
- Hazard, C., Mackey, M. B., & Shimmins, A. J. 1963, Nature, 197, 1040
- Henstock, D. R., *et al.* 1995, ApJS, 100, 1-36

- Impey, C. D., & Tapia, S. 1988, *ApJ*, 333, 666-672
- Impey, C. D., & Tapia, S. 1990, *ApJ*, 354, 124-139
- Impey, C. D. 1992, in *Variability of Blazars*, eds. E. Valtaoja and M. Valtonen (Cambridge University Press, Cambridge), 55-69
- Jauncey, D. L., Batty, M. J., Wright, A. E., Peterson, B. A., & Savage, A. 1984, *ApJ*, 286, 498-502
- Keel, W. C. 1986, *ApJ*, 302, 296-305
- Kellermann, K. I., *et al.* 1971, *ApJ*, 169, 1-25
- Ledden, J. E., & O'Dell, S. L. 1985, *ApJ*, 298, 630-643
- Linfield, R. P., *et al.* 1989, *ApJ*, 336, 1105-1112
- Linfield, R. P., *et al.* 1990, *ApJ*, 358, 350-358
- Lin, Y. C., *et al.* 1995, *ApJ*, 442, 96-104
- Luna, H. G., Martinez, R. E., Combi, J. A., & Romero, G. E. 1993, *A&A*, 269, 77-82
- Lynds, C. R. 1967, *ApJ*, 147, 837-840
- Macchetto, F., *et al.* 1991, *ApJ*, 369, L55-L57
- Maraschi, L., Schwartz, D. A., Tanzi, E. G., & Treves, A., 1985, *ApJ*, 294, 615-618
- Marshall, H. L., Fruscione, A., & Carone, T. E. 1995, *ApJ*, 439, 90-97
- Mattox, J. R., Schachter, J., Molnar, L., Hartman, R. C., & Patnaik, A. R. 1997, *ApJ*, 481, 95-115
- Mead, A. R. G., Ballard, K. R., Brand, P. W. J. L., Hough, J. H. Brindle, C. & Bailey, J. A. 1990, *A&AS*, 83, 183-204
- Moellenbrock, G. A., *et al.* 1996, *AJ*, 111, 2174
- Moore, R. L., & Stockman, H. S. 1981, *ApJ*, 243, 60-75
- Morabito, D. D., Niell, A. E., Preston, R. A., Linfield, R. P., Wehrle, A. E., & Faulkner, J. 1986, *AJ*, 91, 1038-1050
- Morganti, R., Killeen, N. E. B., & Tadhunter, C. N. 1993, *MNRAS*, 263, 1023-1048
- Morton, D. C., Savage, A., & Bolton, J. G. 1978, *MNRAS*, 185, 735-740
- Neff, S. G., Hutchings, J. B., & Gower, A. C. 1989, *AJ*, 97, 1291-1305
- Neugebauer, G., Miley, G. K., Soifer, B. T., & Clegg, P. E. 1986, *ApJ*, 308, 815-828
- O'Dea, C. P., Baum, S. A., & Stanghellini, C. 1991, *ApJ*, 380, 66-77
- Padrielli, L., *et al.* 1986, *A&A*, 165, 53-75

- Pearson, T. J., & Readhead, A. C. S. 1988, ApJ, 328, 114-142
- Perley, R. A. 1982, AJ, 87, 859-880
- Peterson, B. A., Jauncey, D. L., Wright, A. E., & Condon, J. J. 1976, ApJ, 207, L5-L8
- Pica, A. J., Smith, A. G., Webb, J. R., Leacock, R. J., Clements, S., & Gombola, P. P. 1988, AJ, 96, 1215-1226
- Pian, E., *et al.* 1996, ApJ, 459, 169-174
- Polatidis, A. G., *et al.* 1995, ApJS, 98, 1-32
- Preston, R. A., Morabito, D. D., Williams, J. G., Faulkner, J., Jauncey, D. L., & Nicolson, G. D. 1985, AJ, 90, 1599-1641
- Preston, R. A., *et al.* 1989, AJ, 98, 1-26
- Quiniento, Z. M., & Cersosimo, J. C. 1993, A&AS, 97, 435-441
- Robertson, D. S., *et al.* 1993, AJ, 105, 353-358
- Rodgers, A. W., & Peterson, B. A. 1977, ApJ, 212, L9-L12
- Romero, G. E., Benaglia, P., & Combi, J. A. 1995, A&A, 301, 33-40
- Romney, J., *et al.* 1984, A&A, 135, 289-299
- Rusk, R. 1990, J. Roy. Astron. Soc. Can., 84, 199-215
- Schmidt, M. 1963, Nature, 197, 1040
- Shen, Z.-Q., *et al.* 1997, AJ, 114, 1999-2015 (Paper I)
- Shen, Z.-Q., Hong, X.-Y., & Wan, T.-S. 1998, Acta Astrophysica Sinica, in press
- Shepherd, M. C., Pearson, T. J., & Taylor, G. B. 1994, BAAS, 26, 987
- Shimmins, A. J., Bolton, J. G., Peterson, B. A., & Wall, J. V. 1971, Astrophys. Lett., 8, 139-143
- Slee, O. B., Sadler, E. M., Reynolds, J. E., & Ekers, R. D. 1994, MNRAS, 269, 928-946
- Smith, H. J., & Hoffleit, D. 1963, Nature, 198, 650-651
- Sparks, W. B., Miley, G. K., & Macchetto, F. 1990, ApJ, 361, L41-L44
- Steppe, H., Salter, C. J., Chini, R., Kreysa, E., Brunswig, W., & Pérez, J. L. 1988, A&AS, 75, 317-351
- Steppe, H., Liechti, S., Mauersberger, R., Kömpe, C., Brunswig, W., & Ruiz-Moreno, M. 1992, A&AS, 96, 441-475
- Steppe, H., *et al.* 1993, A&AS, 102, 611-635
- Stickel, M., Fried, J. W., & Kühr, H. 1989, A&AS, 80, 103-114

- Stickel, M., Padovani, P., Urry, C. M., Fried, J. W., & Kühr, H. 1991, ApJ, 374, 431-439
- Stickel, M., Fried, J. W., & Kühr, H. 1993, A&AS, 98, 393-442
- Strittmatter, P. A., Serkowski, K., Carswell, R., Stein, W. A., Merrill, K. M., & Burbidge, E. M. 1972, ApJ, 175, L7-L13
- Swanenburg, B. N., *et al.* 1978, Nature, 275, 298
- Tanzi, E. G., *et al.* 1986, ApJ, 311, L13-L16
- Taylor, G. B., *et al.* 1994, ApJS, 95, 345-369
- Thakkar, D. D., *et al.* 1995, ApJS, 98, 33-40
- Thompson, D. J., *et al.* 1993a, ApJ, 410, 87-89
- Thompson, D. J., *et al.* 1993b, ApJ, 415, L13-L16
- Thompson, D. J., *et al.* 1995, ApJS, 101, 259-286
- Tingay, S. J., *et al.* 1996, ApJ, 464, 170-176
- Tornikoski, M., Valtaoja, E., Teräsanta, H., Lainela, M., Bramwell, D., & Botti, L. C. L. 1993, AJ, 105, 1680-1689
- Treves, A., *et al.* 1993, ApJ, 406, 447-450
- Ulvestad, J. S., Johnston, K. J., & Weiler, K. W. 1983, ApJ, 266, 18-27
- Unwin, S. C. *et al.* 1985, ApJ, 289, 109-119
- Urry, C. M., & Padovani, P. 1995, PASP, 107, 803-845
- Vermeulen, R. C. & Cohen, M. H. 1994, ApJ, 430, 467-494
- von Montigny, C., *et al.* 1995, ApJ, 440, 525-553
- Wall, J. V., Danziger, I. J., Pettini, M., Warwick, R. S., & Wamsteker, W. 1986, MNRAS, 219, 23-29
- Wardle, J. F. C., Moore, R. L., & Angel, J. R. P. 1984, ApJ, 279, 93-111
- Webb, J. R., Smith, A. G., Leacock, R. J., Fitzgibbons, G. L., Gombola, P. P., & Shepherd, D. W. 1988, AJ, 95, 374-397
- Wehrle, A. E., Cohen, M. H., Unwin, S. C., Aller, H. D., Aller, M. F., & Nicolson, G. 1992, ApJ, 391, 589-607
- Weiler, K. W., & de Parter, I. 1983, ApJS, 52, 293-327
- Weiler, K. W., & Johnston, K. J. 1980, MNRAS, 190, 269-285
- White, G. L., *et al.* 1988, ApJ, 327, 561-569

- Wilkes, B. J., Wright, A. E., Jauncey, D. L., & Peterson, B. A. 1983, *Proc. Astron. Soc. Australia*, 5, 2-9
- Wilkes, B. J. 1986, *MNRAS*, 218, 331-361
- Wilkes, B. J., Elvis, M., Fiore, F., McDowell, J. C., Tananbaum, H., & Lawrence, A. 1992, *ApJ*, 393, L1-L4
- Wills, B. J., & Browne, I. W. A. 1986, *ApJ*, 302, 56-63
- Wills, B. J., Wills, D., Breger, M., Antonucci, R. R. J., & Barvainis, R. 1992, *ApJ*, 398, 454-475
- Wright, A., Peterson, B. A., Jauncey, D. L., & Condon, J. J. 1979, *ApJ*, 229, 73-77
- Wright, A., Ables, J. G., & Allen, D. A. 1983, *MNRAS*, 205, 793-807
- Xu, W., Readhead, A. C. S., Pearson, T. J., Polatidis, A. G., & Wilkinson, P. N. 1995, *ApJS*, 99, 297-348
- Zensus, J. A. 1987, in *Superluminal Radio Sources*, eds. J. A. Zensus and T. J. Pearson (Cambridge University Press, Cambridge), 26-31
- Zensus, J. A., Bååth, L. B., Cohen, M. H., & Nicolson, G. D. 1988, *Nature*, 334, 410-412

FIGURE CAPTION

Fig. 1— VLBI images of the 23 extragalactic radio sources observed in May 1993. The synthesized beam is shown in the lower left of each image. See Table 3 for detailed imaging parameters.

TABLE 2. Antenna Characteristics in 1993 May

Station Location (Code) (1)	Diameter (m) (2)	η (%) (3)	T_{sys} (Jy) (4)	Gain (K/Jy) (5)	Pol (6)	Frequency Standard (7)
Hartebeesthoek (E)	26.0	52	970	0.100	LCP	H-Maser
Hobart (Hb)	26.0	52	1700	0.100	LCP	H-Maser
Mopra (M)	22.0	62	500	0.086	LCP	Rubidium
Parkes (P)	64.0	43	130	0.500	LCP	H-Maser
Perth (Pr)	27.5	47	1400	0.100	LCP	Rubidium
Shanghai (Sh)	25.0	56	2000	0.100	LCP	H-Maser

Notes to Table 2.

- (1) Station name and antenna code in parentheses.
- (2) Antenna diameter.
- (3) Effective antenna aperture efficiency.
- (4) System temperature.
- (5) System gain factor.
- (6) Polarization, IEEE convention.
- (7) Type of frequency standard used.

TABLE 3. Source Map Descriptions

Source Name (1)	S_{peak} (Jy/Beam) (2)	Restoring Beam			Contours (Jy/Beam) (6)	Scale (pc/mas) (7)	VLBI Morphology (mas scale) (8)
		Major (mas) (3)	Minor (mas) (4)	P.A. (deg) (5)			
PKS 0118–272	0.33	3.6	1.9	–1	$0.012 \times (-1, 1, 2, \dots, 16)$	3.7	single core
PKS 0208–512	2.38	2.2	1.1	–12	$0.015 \times (-1, 1, 2, \dots, 128)$	4.3	core–jet
PKS 0332–403	0.85	1.4	1.1	–10	$0.006 \times (-1, 1, 2, \dots, 64)$	4.3	core–jet
PKS 0403–132	0.77	1.4	1.1	21	$0.006 \times (-1, 1, 2, \dots, 64)$	3.7	single core
PKS 0426–380	0.67	1.7	1.2	16	$0.006 \times (-1, 1, 2, \dots, 64)$	4.3	single core
PKS 0438–436	1.08	1.7	1.0	4	$0.015 \times (-1, 1, 2, \dots, 64)$	3.7	core–jet
PKS 0454–234	1.79	3.5	1.5	71	$0.012 \times (-1, 1, 2, \dots, 128)$	4.3	core–jet
PKS 0521–365	1.34	1.9	1.0	10	$0.006 \times (-1, 1, 2, \dots, 128)$	0.7	core–jet
PKS 0537–441	2.82	2.7	1.1	13	$0.018 \times (-1, 1, 2, \dots, 128)$	4.2	core–jet
PKS 0823–223	0.30	2.5	1.7	8	$0.003 \times (-1, 1, 2, \dots, 64)$	4.2	single core
PKS 1034–293	1.12	1.5	1.1	17	$0.009 \times (-1, 1, 2, \dots, 64)$	2.8	single core
PKS 1127–145	1.35	2.8	1.4	69	$0.009 \times (-1, 1, 2, \dots, 128)$	4.3	core–jet
PKS 1226+023	12.70	1.2	0.9	33	$0.054 \times (-1, 1, 2, \dots, 128)$	1.8	core–jet
PKS 1244–255	1.43	1.6	1.0	8	$0.015 \times (-1, 1, 2, \dots, 64)$	3.9	single core
PKS 1424–418	0.96	2.3	1.1	–2	$0.012 \times (-1, 1, 2, \dots, 64)$	4.3	core–jet
PKS 1514–241	1.10	2.0	1.0	5	$0.024 \times (-1, 1, 2, \dots, 32)$	0.7	single core
PKS 1936–155	0.84	2.4	1.0	6	$0.006 \times (-1, 1, 2, \dots, 128)$	4.2	single core
PKS 1954–388	1.79	2.1	1.1	26	$0.006 \times (-1, 1, 2, \dots, 256)$	3.9	single core
PKS 2005–489	0.77	2.7	1.5	–9	$0.009 \times (-1, 1, 2, \dots, 64)$	0.9	single core
PKS 2155–152	1.48	2.1	1.4	62	$0.015 \times (-1, 1, 2, \dots, 64)$	3.9	core–jet
PKS 2240–260	0.35	1.5	1.1	10	$0.006 \times (-1, 1, 2, \dots, 32)$	4.1	core–jet
PKS 2243–123	1.62	1.4	1.0	9	$0.021 \times (-1, 1, 2, \dots, 64)$	3.9	single core
PKS 2355–534	1.31	2.8	1.2	20	$0.009 \times (-1, 1, 2, \dots, 128)$	4.3	core–jet

Notes to Table 3.

- (1) Source name.
- (2) Peak flux density.
- (3), (4), (5) Parameters of the restoring Gaussian beam: Full Width at Half Maximum (FWHM) of the major and minor axes and the position angle (P.A.) of the major axis.
- (6) Contour levels of the map, starting from 3 times the rms value in the image ('...' means a factor of 2 between adjacent contours).
- (7) Angular size scale (with $H_0 = 100 \text{ km s}^{-1} \text{ Mpc}^{-1}$ and $q_0 = 0.5$).
- (8) Apparent morphology of the source.

TABLE 4. Source Model Descriptions

Source Name (1)	Component Number (2)	S (Jy) (3)	r (mas) (4)	ϕ (deg) (5)	Gaussian Model			Brightness Temperature (10^{12} K) (9)
					Major (mas) (6)	Minor (mas) (7)	P.A. (deg) (8)	
PKS 0118–272	1	0.55	0.00	0	3.8	1.5	1	0.007
PKS 0208–512	1	2.77	0.00	0	0.6	0.2	73	1.90
	2	0.27	1.70	234	1.4	0.8	42	0.02
PKS 0332–403	1	1.28	0.00	0	1.0	0.2	106	0.64
	2	0.06	1.97	103	0.2	0.1	87	0.24
PKS 0403–132	1	0.85	0.00	0	0.5	0.3	151	0.50
PKS 0426–380	1	0.84	0.00	0	0.6	0.2	111	0.69
PKS 0438–436	1	1.42	0.00	0	0.7	0.5	119	0.78
	2	0.99	36.38	135	6.6	4.6	3	0.006
	3	0.38	6.57	122	3.6	2.4	103	0.008
PKS 0454–234	1	2.04	0.00	0	0.8	0.4	163	0.61
	2	0.10	2.37	318	1.0	0.6	88	0.02
PKS 0521–365	1	1.82	0.00	0	0.9	0.6	135	0.17
	2	0.20	3.38	320	0.9	0.4	170	0.03
	3	0.22	8.27	315	3.8	2.0	142	0.001
PKS 0537–441	1	3.37	0.00	0	0.9	0.4	75	0.86
	2	0.28	2.61	14	1.3	0.8	91	0.02
PKS 0823–223	1	0.40	0.00	0	1.2	0.3	124	0.12
PKS 1034–293	1	1.54	0.00	0	0.8	0.5	102	0.26
PKS 1127–145	1	1.91	0.00	0	1.6	1.0	81	0.13
	2	1.12	3.23	265	1.8	0.5	87	0.13
PKS 1226+023	1	21.80	0.00	0	1.2	0.5	66	2.04
	2	2.91	1.87	215	0.8	0.5	162	0.38
	3	2.84	3.81	232	0.7	0.2	127	1.29
	4	4.50	7.12	231	1.4	1.2	54	0.14
	5	0.97	8.69	230	0.6	0.2	62	0.55
	6	2.23	15.24	235	2.5	1.0	66	0.05
PKS 1244–255	1	1.75	0.00	0	0.7	0.4	116	0.56
PKS 1424–418	1	1.36	0.00	0	0.9	0.7	67	0.25
	2	0.12	2.74	260	1.1	0.4	2	0.04

TABLE 4. (continued)

Source Name (1)	Component Number (2)	S (Jy) (3)	r (mas) (4)	ϕ (deg) (5)	Gaussian Model			Brightness Temperature (10^{12} K) (9)
					Major (mas) (6)	Minor (mas) (7)	P.A. (deg) (8)	
PKS 1514–241	1	1.53	0.00	0	1.2	0.6	177	0.11
PKS 1936–155	1	0.97	0.00	0	0.6	0.5	176	0.47
PKS 1954–388	1	1.94	0.00	0	0.4	0.3	82	1.20
PKS 2005–489	1	0.92	0.00	0	1.0	0.2	71	0.26
PKS 2155–152	1	2.10	0.00	0	1.8	0.1	34	0.67
	2	0.23	4.21	15	1.1	0.3	26	0.05
PKS 2240–260	1	0.54	0.00	0	1.0	0.5	125	0.10
	2	0.12	2.21	314	1.3	0.1	7	0.08
PKS 2243–123	1	2.28	0.00	0	1.1	0.4	175	0.40
PKS 2355–534	1	1.54	0.00	0	1.1	0.4	31	0.35
	2	0.20	4.88	235	1.1	0.6	66	0.03

Notes to Table 4.

- (1) Source name.
- (2) Numerical label, component 1 is assumed to be the core.
- (3) Flux density of each component.
- (4) Distance of each component from the origin defined by component 1.
- (5) Position angle of each component with respect to the origin.
- (6), (7) and (8) Parameters of Gaussian model: major and minor axes of each component (FWHM) and the position angle (P.A.) of the major axis.
- (9) Peak brightness temperature.

TABLE 5. Summary of Source Position Angles at Arcsecond and Milliarcsecond Scales

Source Name	Optical Type ^a	P.A. Arcsec. Scale (degree)	P.A. mas Scale (degree)	P.A. Difference (degree)	EGRET Source
PKS 0118-272	B	diffused	N/A	...	Y
PKS 0208-512	Q	225	234	9	
PKS 0332-403	Q	unresolved	103	...	
PKS 0403-132	Q	23	45	22	
PKS 0426-380	B	336	N/A	...	
PKS 0438-436	Q	15	122	107	
PKS 0454-234	B	N/A	318	...	Y?
PKS 0521-365	B	302	320	18	Y
PKS 0537-441	B	305	14	69	Y
PKS 0823-223	B	diffused	N/A	...	
PKS 1034-293	B	N/A	N/A	...	
PKS 1127-145	Q	41	265	136	Y
PKS 1226+023	Q	222	230	8	Y
PKS 1244-255	Q	N/A	N/A	...	
PKS 1424-418	Q	350	260	90	Y
PKS 1514-241	B	120	N/A	...	
PKS 1936-155	Q	unresolved	N/A	...	
PKS 1954-388	Q	diffused	N/A	...	
PKS 2005-489	B	N/A	N/A	...	Y?
PKS 2155-152	B	0	15	15	
PKS 2240-260	B	N/A	314	...	
PKS 2243-123	Q	40	180	140	
PKS 2355-534	Q	N/A	235	...	

^a B = BL Lac Object, Q = Quasar.